Microtubule Behavior during Guidance of Pioneer Neuron Growth Cones in situ

James H. Sabry, Timothy P. O'Connor,* Louise Evans, Alma Toroian-Raymond,* Marc Kirschner, and David Bentley*

Department of Biochemistry and Biophysics, University of California, San Francisco, California 94143; and *Department of Molecular and Cell Biology, University of California, Berkeley, California 94720

Abstract. The growth of an axon toward its target results from the reorganization of the cytoskeleton in response to environmental guidance cues. Recently developed imaging technology makes it possible to address the effect of such cues on the neural cytoskeleton directly. Although high resolution studies can be carried out on neurons in vitro, these circumstances do not recreate the complexity of the natural environment.

We report here on the arrangement and dynamics of microtubules in live neurons pathfinding in response to natural guidance cues in situ using the embryonic grasshopper limb fillet preparation. A rich microtubule network was present within the body of the growth cone and normally extended into the distal growth cone margin. Complex microtubule loops often formed transiently within the growth cone. Branches both with and without microtubules were regularly observed. Microtubules did not extend into filopodia.

During growth cone steering events in response to identified guidance cues, microtubule behaviour could be monitored. In turns towards guidepost cells, microtubules selectively invaded branches derived from filopodia that had contacted the guidepost cell. At limb segment boundaries, microtubules displayed a variety of behaviors, including selective branch invasion, and also invasion of multiple branches followed by selective retention in branches oriented in the correct direction. Microtubule invasion of multiple branches also was seen in growth cones migrating on intrasegmental epithelium. Both selective invasion and selective retention generate asymmetrical microtubule arrangements within the growth cone, and may play a key role in growth cone steering events.

DEVELOPING neurons may send their processes over great distances and through complex environments to establish contact with their target cells (Caudy and Bentley, 1986*b*; Dodd and Jessell, 1988; Goodman et al., 1984; Harris et al., 1987; O'Leary and Terashima, 1988; Tosney and Landmesser, 1985; Westerfield and Eisen, 1988). This outgrowth is not random but, rather, is guided by environmental cues. It has long been appreciated that neuronal guidance can essentially be viewed as the process by which the growth cone, the dynamic and expanded tip of the neurite, is oriented by environmental cues (Harrison, 1910). These cues appear to be provided by a variety of factors, including substrate-bound molecules on cell surfaces and in the extracellular matrix, and diffusible chemoattractant molecules (Anderson, 1988; Elkins et al., 1990; Fessler and Fessler, 1989; Goodman et al., 1984; Reichardt and Tomaselli, 1991; Tessier-Lavigne and Placzek, 1991). The arrangement of these factors in the developing embryo presumably provides the information necessary to guide the developing neurons. In order for growth cones to reach their targets, they must alter their direction of growth in response to these factors, a process termed steering.

The process of growth cone steering first involves the exploration of the environment by growth cone filopodia, lamellipodia and branches to locate discrete guidance cues or to evaluate the spatial distribution of cues in the region around the growth cone (Bentley and Toroian-Raymond, 1986; Bray and Hollenbeck, 1988; Goldberg and Burmeister, 1989; Mitchison and Kirschner, 1988). A subset of filopodia, lamellipodia, or branches are then selected for the direction of further growth cone extension. This is followed by the intrusion of cellular material into the selected process, resulting in growth cone reorientation (Aletta and Greene, 1988; Goldberg and Burmeister, 1986; Heidemann et al., 1984). These cellular components are subsequently consolidated into a stable configuration characteristic of the axon (Hirokawa et al., 1988; Lewis et al., 1989).

Many cellular components, including cytoskeletal elements such as microtubules and actin filaments, and intracellular second messenger molecules, are likely to be involved in the directed growth of axons (Goldberg and Burmeister, 1989; Kater and Mills, 1991; Lankford and Letourneau, 1989; Meininger and Binet, 1989). It is not known whether

J. H. Sabry and T. P. O'Connor contributed equally to the experiments in this paper.

environmental cues directly affect all these components, but oriented axonal growth ultimately must alter the arrangement of cytoskeletal polymers within the axon. Indeed, the generation of an asymmetric arrangement of microtubules may be a key event in growth cone steering. This can be accomplished by two mechanisms: (*a*) selective microtubule invasion of a limited region of the growth cone; or (*b*) random invasion of many regions of the growth cone followed by selective retention of microtubules extended in the direction of future growth. Recently, direct observations of microtubules in living *Xenopus* growth cones in vitro have identified microtubule behaviors that may underlie steering decisions (Tanaka and Kirschner, 1991). However, it is not known which, if any, of these behaviors play a role in pathfinding in the complex environment of the embryo.

In order to address this issue, we characterized the dynamic behavior of microtubules in response to in situ guidance cues by imaging fluorescently labeled microtubules in Til pioneer neurons in live grasshopper embryonic limb fillets. In the grasshopper embryo, a pair of sibling neurons, termed the Til pioneers, are the first neurons to extend axons toward the central nervous system (Bate, 1976; Bentley and Keshishian, 1982; Ho and Goodman, 1982). They are born at the distal tip of the limb bud, emerge on the basal surface of the epithelium, and extend growth cones proximally along the limb axis. As they migrate, the growth cones contact a complex environment consisting of epithelial cells, basal lamina and pre-axonogenesis neurons termed "guidepost cells" (Anderson and Tucker, 1988; Caudy and Bentley, 1986*b*; Condic and Bentley, 1989*b*; Lefcort and Bentley, 1987). The pathway taken by the Til growth cones is illustrated in Fig. 1. Key regions of the pathway, where distinctive growth cone behaviors occur, are enclosed in the series of boxes. Box 1 shows a growth cone in the femur, where it interacts primarily with intrasegmental epithelial cells and the overlying basal lamina. In this region, growth cones migrate proximally along the limb axis with frequent small course corrections. Box 2 shows the growth cones spreading on the Tr1 guidepost cell at the Tr-Cx segment boundary. At this location, the growth cones encounter two orthogonally arranged bands of limb segment boundary cells, a distal band of high adhesivity cells (see Fig. 1, *filled hexagons*), and a proximal band of lower adhesivity cells shown by the unfilled hexagons in Fig. 1 (Bastiani et al., 1991; Caudy and Bentley, 1987; Condic and Bentley, 1989*a*). The growth cones extend branches both dorsally (up in all figures) and ventrally on the first band of cells, but eventually always make a ventral turn. Box 3 shows the growth cones migrating ventrally along the Tr-Cx segment boundary and approaching the Cx1 guidepost cells. When a growth cone filopodium contacts the Cx1 cells, the growth cone turns along it, by a process of filopodial dilation, toward the CNS (O'Connor et al., 1990).

The Til pathway in the embryonic grasshopper limb can be rendered accessible for manipulation using an opened epithelial "fillet" preparation (Lefcort and Bentley, 1987). This exposes the Til cell bodies, but preserves the guidance information present in the limb, and allows the growth cones to be imaged as they migrate proximally. In the experiments reported here, we injected the Til neuron with rhodamine-conjugated bovine tubulin and imaged the labeled microtubules using a cooled charge-coupled device (CCD) camera system (Castleman, 1979; Hiraoka et al., 1987). The arrangement of microtubules in growth cones migrating in a complex environment, and how they respond during pathfinding decisions, could be examined. In particular, we determined where microtubules are present in growth cones in situ, and how their arrangement changes over time as steering decisions are made. We also investigated whether microtubule rearrangements are different during steering events at different locations along the pathway. This approach revealed novel aspects of microtubule behavior that address the mechanism of growth cone steering.

Materials and Methods

Grasshopper Embryos and Dissection

Schistocerca americana embryos were obtained from the University of California at Berkeley grasshopper colony. Eggs at the 31–34% stages of embryonic development were sterilized and the embryos dissected as previously described (Lefcort and Bentley, 1987). The embryos were transferred to a poly-L-lysine–coated coverslip and maintained in supplemented RPMI (Condic and Bentley, 1989*a*). Briefly, the embryos were positioned ventral side down, thus exposing the posterior aspect of the limb bud. This surface was cut along the long axis of the limb, and the sides unrolled and flattened out onto the coverslip. The exposed interior mesodermal cells were removed using a suction pipette, leaving the basal lamina and epithelium-derived cells. The Til neuronal cell bodies were visualized with differential interference contrast optics using a Nikon inverted compound microscope.

Fluorescent Labeling of Tubulin

Purified bovine brain tubulin was labeled with tetramethyl-rhodamine as previously described (Hyman et al., 1991). This process involved covalently linking the N-hydroxyl succinimidyl ester of tetramethyl-rhodamine (#C-1171; Molecular Probes, Eugene, OR) to purified bovine brain tubulin. The labeled tubulin was then subjected to two cycles of temperature-dependent assembly/disassembly to select for assembly competent tubulin. The labeled tubulin was stored at a concentration of 20–30 mg/ml in an injection buffer (50 mM K glutamate, 0.5 mM $MgCl_2$, pH 6.5) at −80°C.

Neuronal Labeling

A Til neuron cell body was injected with rhodamine-conjugated bovine tubulin using a pulled, bevelled borosilicate micropipette. Selected cells were also double labeled with the carbocyanine dye, DiO (1,1'-dihexadecyloxacarbocyanine perchorate, $DiOC_{16}$, #D-1125; Molecular Probes) as previously described (O'Connor et al., 1990). Briefly, this involved air drying the DiO onto the tip of a pulled micropipette, and labeling the cell by gently touching it with the micropipette.

Microtubule Imaging and Analysis

Most imaging, including the images selected for the figures, was done at the Berkeley Low-light-level Video Center using a cooled charge-coupled device (CCD) camera system (Photometrics; Tuscon, AZ). This system comprised viewing the fluorescent tissue through a 100X, 1.4 NA Nikon objective on a Nikon inverted compound microscope with conventional relay optics connecting the microscope to the CCD camera. The microscope projected the image onto a 1320 × 1024 pixel chip Kodak (KAF-1400), which digitized the image and transferred the data to a bulk memory storage device (REO-650 erasable optical disc; Pinnacle Micro, Inc., Irvine, CA). Image space on the chip was 0.06 μm/pixel. The chip, light path shutters, and stage focal position were controlled by a Perceptics BioVision imaging system (Knoxville, TN) on a Mac IIx computer (Apple Computers, Cupertino, CA). Illumination was provided by a 100 W mercury lamp, generally in 300–400 ms exposures. To image the full thickness of the growth cone, five to eight optical sections were usually taken. Clusters of sections were usually taken every 4 to 8 min. On occasion, images were taken every 3 s to resolve high frequency events. By tracking fluorescence through multiple image planes, out-of-focus fluorescence was identified and reduced using Focus software (Vaytek; Fairfield, IA). Microtubules traversing multiple sections were montaged with National Institutes of Health Image software. Processed images were photographed directly from a 1280 × 1024

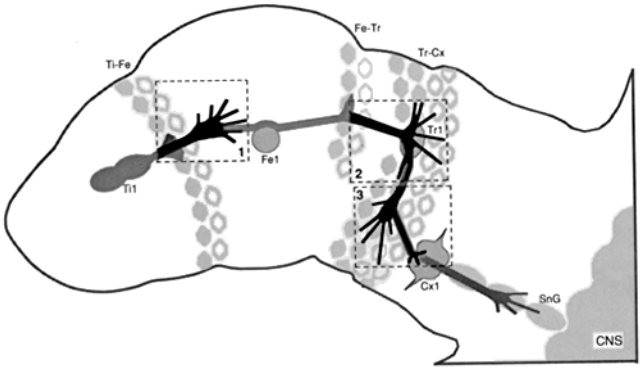

Figure 1. A diagram of the Til pioneer neuron pathway in the embryonic grasshopper limb bud at the 35% stage. The pair of sibling Til neurons arise at the limb tip and their growth cones migrate to the central nervous system (*CNS*) along a stereotyped route. The growth cone route reflects a series of steering decisions resulting from encounters with guidance cues. These include preaxonogenesis ("guidepost") neurons (*Fel*, *Trl*, *Cxl*), high affinity (*filled hexagons*) and low affinity (*unfilled hexagons*) circumferential bands of epithelial cells at limb segment boundaries (*Ti-Fe*, *Fe-Tr*, *Tr-Cx*), and segmental nerve-root glial cells (*SnG*). The dashed boxes (*1–3*) indicate limb regions where growth cone microtubule behavior is illustrated in other figures. *Ti-Fe*, tibia-femur boundary; *Fe-Tr*, femur-trochanter boundary; *Tr-Cx*, trochanter-coxa boundary. The length of the leg is approximately 350 μm. Dorsal, up; proximal, to right.

pixel video-screen (E-Machines, Beaverton, OR). Using a system developed by Drs. John Sedat and David Agard (Department of Biochemistry, University of California at San Francisco), additional images were visualized on an inverted Olympus IMT-2 microscope connected to a peltier cooled CCD (Photometrics, Tucson, AZ) equipped with a 900 × 900 pixel chip (Texas Instruments), and controlled by a Microvax II workstation (Digital Equipment Corp., Marlboro, MA).

EM Microscopy

After imaging, selected embryos were prepared for EM. This involved fixing them in 2% glutaraldehyde in PBS for 4 h at room temperature. They were then reacted with a primary serum antibody (against HRP) that recognizes insect neurons (Jan and Jan, 1982; Snow et al., 1987). This antibody was visualized using a 10 nm gold conjugated secondary antibody (Amersham, UK). After a second fixation in 2% glutaraldehyde in PBS, the tissue was rinsed and osmicated in 2% OsO_4 in cacodylate buffer for 30 min. The labeled tissue was then dehydrated rapidly through an ethanol series, and embedded in araldite (Grade CY-212 British, Polysciences, Warrington, PA). The Til pioneer neuron was first identified in thick sections at the light microscopic level by silver enhancing the gold particles (Amersham, UK). Thin sections were then cut and observed in a Phillips 400 electron microscope (80 kV).

Results

To observe microtubules in growing neurons, we flattened out the tubular limb bud, bathed it in culture medium, injected the Til pioneer neuron, and exposed it to brief pulses of visible light. Under these conditions, the route taken by the Til growth cone was indistinguishable from that of the neuron in vivo. This suggests not only that natural in vivo guidance cues are preserved in the fillet, but also that the incorporation and subsequent imaging of rhodamine-conjugated bovine tubulin has little effect on the pattern of Til axonal growth.

The Til pioneer neurons are siblings, and only one of each pair was injected for these studies. Although the two neurons are strongly coupled by dye-passing junctions (Keshishian and Bentley, 1983; Taghert et al., 1982), no label was ever found to cross to the noninjected cell, implying that no unconjugated free rhodamine dye was generated by proteolysis of the labeled monomer. The label traveled down the axon and was found to persist as a low level of background fluorescence, thought to represent monomeric rhodamine-tubulin, and in clearly defined linear tracks in the axon and growth cone. An example of these tracks is illustrated in Fig. 2 which shows a rich network of linear tracks in the growth cone. A single track invading a branch is shown by the arrowhead. We measured the width and intensity of the tracks in this and other cells. The image width of these tracks, which we will refer to as microtubules, was found to be very uniform (0.24 μm; SEM, 0.01 μm, mean of 15; three measurements per microtubule, three microtubules per cell in five cells at various stages of development). This value is similar to published widths of fluorescent images of electron microscope–confirmed single microtubules (Sammak and Borisy, 1988). More importantly, although the pixel intensity of these linear profiles varied significantly from cell to cell, within a given cell all profiles were of similar intensity. For instance, in the growth cone shown in Fig. 2, the mean intensity of five tracks (five measurements per track) was 91.6 U with an SEM = 2.7 (2.9%). This represented a value in the middle of the dynamic range of the CCD chip which was

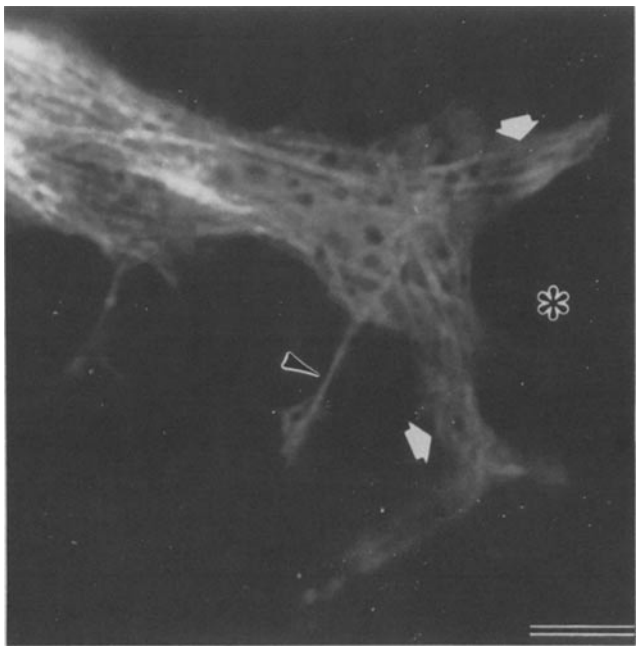

Figure 2. Microtubule arrangements in a pioneer growth cone spreading on guidepost cell Trl. A Til pioneer neuron has been injected with rhodamine-tubulin and the growth cone is at the Trl cell (*asterisk*). This position corresponds to Fig. 1, *box 2*. Many uniform caliber linear fluorescent tracks, which appear to be single microtubules (see text), are observed. Although the growth cone will eventually turn ventrally at this location, microtubules are present in branches (*white arrows*) extending both dorsally and ventrally along the Tr-Cx segment boundary. A single microtubule (*arrowhead*) is present in a ventrally extended branch. Bar, 5 μm.

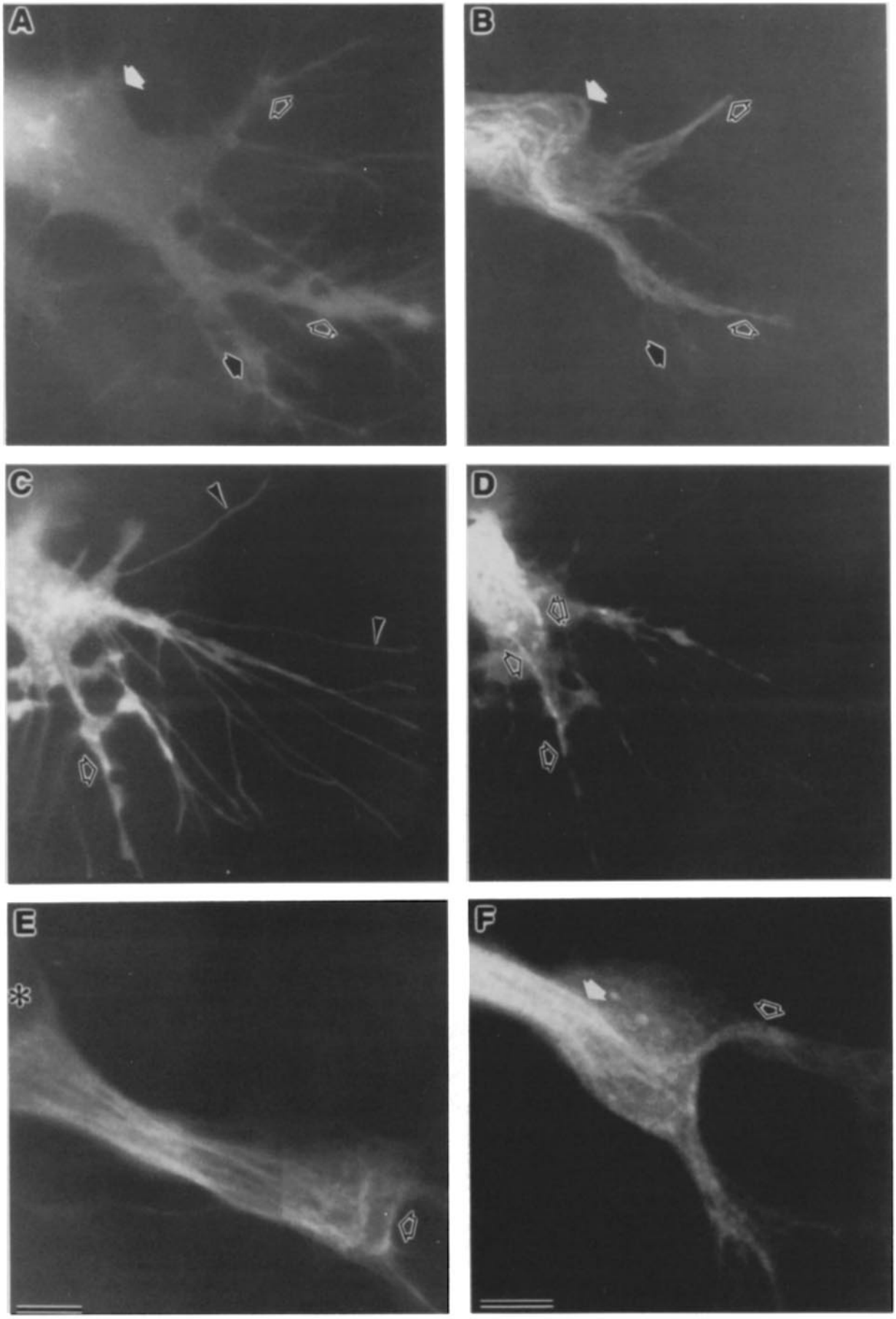

0–255 U. As detailed below, EM identified many single microtubules in the distal growth cone. These data strongly suggest that these fluorescent tracks represent single microtubules. The label persisted for ~7 h, and then slowly faded, probably as a result of tubulin turnover.

The Arrangement of Microtubules in Til Neurons

In 31 embryos, 31 Til growth cones were imaged in which microtubules were clearly resolved. These images were obtained at various places in the pathway, with most observations at the turning decisions outlined by the boxes in Fig. 1. To visualize the full extent of the growth cone and its processes, eight growth cones were simultaneously labeled with a lipophilic carbocyanine membrane dye, DiO.

Axons. In all neurons imaged, the microtubules were found in the axon cylinder in closely packed linear arrays. This can be appreciated in Fig. 3 *F*, where the microtubules in the upper left of the panel were found oriented along the long axis of the neuron and were closely bundled together. The plasma membrane was closely apposed to the microtubule array. Other examples of the arrangement of microtubules in axons can be seen in Figs. 2, 3 *E*, 4, 7, and 8. Occasionally, at locations of laterally extended protrusions, the plasma membrane was not closely apposed to the microtubule bundle, and some microtubule free axoplasm could be visualized (data not shown).

The morphologic boundary between the axon and growth cone can usually be defined when neurons are viewed in vitro as that region where the axonal cylinder abruptly increases in caliber (Bray and Chapman, 1985; Goldberg and Burmeister, 1986). However, in situ, this border could not easily be identified by plasma membrane morphology in many Til neurons. In these cases, no abrupt transition from the cylindrical shape of the axon to the globular shape of the growth cone was evident. However, in some neurons, the arrangement of microtubules did show an unambiguous transition from the tightly bundled arrangement characteristic of axons to a rich network of single or small bundles of microtubules characteristic of the growth cone. For example, Fig. 3 *F* shows microtubules in a growth cone of this type; the white arrow indicates the transition from the bundled microtubule array of the axon, to the left of the white arrow, to the more dispersed arrangement of the growth cone, to the right.

Growth Cones. All growth cones were heavily invested with microtubules. In all cases, microtubules were found to inhabit the distal region of the growth cone, up to the plasma membrane. In Fig. 2, for instance, a rich network of microtubules can be seen in the whole growth cone. In this figure, the edge of the growth cone was indicated by the background level of fluorescence. In Fig. 3 *E*, microtubules (indicated by the *unfilled arrow*) seem to have extended directly underneath the distalmost aspect of the growth cone plasma membrane. Microtubules were not restricted to the central portion of the growth cone for prolonged periods of time, as has been described for some types of neurons in vitro (Bridgman and Daily, 1989; Forscher and Smith, 1988). In contrast to the axon, growth cone microtubules were not restricted to tight bundles, but frequently occurred singly or as small bundles. In several neurons, images were taken every three seconds; rapid shrinkage and regrowth of microtubules was not apparent.

In the fillet, although the cell body could be identified by DIC optics, the growth cone could only be visualized using epifluorescence. Many protrusions, particularly branches, could be identified by the presence of background fluorescence; however, as it was not clear that all the fine structure of the growth cone could be seen, eight growth cones were double labeled with the lipophilic plasma membrane dye, DiO. As has been described previously (O'Connor et al., 1990), we observed extensive and varied protrusive activity from the growth cone. Types of protrusions included: (*a*) filopodia: fine, tubular structures of a single uniform caliber that arise from the growth cone or from branches; (*b*) veils and lamellipodia: thin sheets that often extend between existing filopodia; and (*c*) branches: elongate processes of variable size and shape that were wider than filopodia, and often tapered from their base to tip.

Filopodia. The Til growth cone is rich in filopodia, which were abundant in all double-labeled growth cones. In total, 150 filopodia were identified on DiO images. In Fig. 3 *C*, many long filopodia (arrowheads) can be seen to have arisen at the distal end of the growth cone. In the imaging plane, the mean number of filopodia per growth cone was 21 with a range from 8 to 34. The mean width was 0.31 μm, with an SEM of 0.015 (4.8%). As was described by O'Connor et al. (1990), some filopodia were very stable and unchanging in length or position over tens of minutes, whereas others were very dynamic, existing for a minute or less. None of the filopodia, even those with long lifetimes, harbored microtubules. This can be seen in Fig. 3 *D*, which is the rhodamine-tubulin image of a double-labeled growth cone (the DiO image is seen in Fig. 3 *C*). The unfilled arrows point to microtubules in the body of the growth cone, and in a branch, but none of the filopodia identified by arrowheads

Figure 3. Microtubule arrangements during growth cone migration on a relatively homogeneous substrate. These positions correspond to Fig. 1, *box 1*. (*A* and *B*) A growth cone double labeled with a lipophilic plasma membrane dye (DiO; *A*), and rhodamine tubulin (*B*). Bundles of microtubules are present in branches extending in different, but generally proximally oriented directions (*A* and *B*, *unfilled arrows*). Microtubules are absent from some branches (*A* and *B*, *black arrow*). Pronounced microtubule loops exist in the growth cone (*A* and *B*, *white arrows*). The sibling neuron was slightly labeled with DiO, and the faint image of the sibling growth cone can be seen in the lower left part of *A*. (*C* and *D*) In another double-labeled growth cone in this region, single microtubules are present in the growth cone periphery (*D*, *double arrow*), and can extend into small branches (*C* and *D*, *unfilled arrows*). Many uniform diameter filopodia extend from the growth cone (*C*, *arrowheads*); these do not contain microtubules. (*E* and *F*) In a nascent growth cone which has migrated a short distance from the cell body (*E*, *asterisk* = nucleus), microtubule bundles form loops against the growth cone perimeter (*E*, *arrow*). 34 min later, these loops have straightened somewhat as the microtubules enter a branch forming dorsally (*F*, *unfilled arrow*). Microtubules also enter a ventral branch which was not selected as the direction of growth cone extension. This growth cone was subsequently imaged by EM shown in Figs. 5 and 6. Within the body of the growth cone, a marked transition zone (*F*, *white arrow*) occurs where dispersed microtubules of the growth cone periphery form into a closely packed axonal array. Bar in F refers to *A–D* and *F*. Bars, 5 μm.

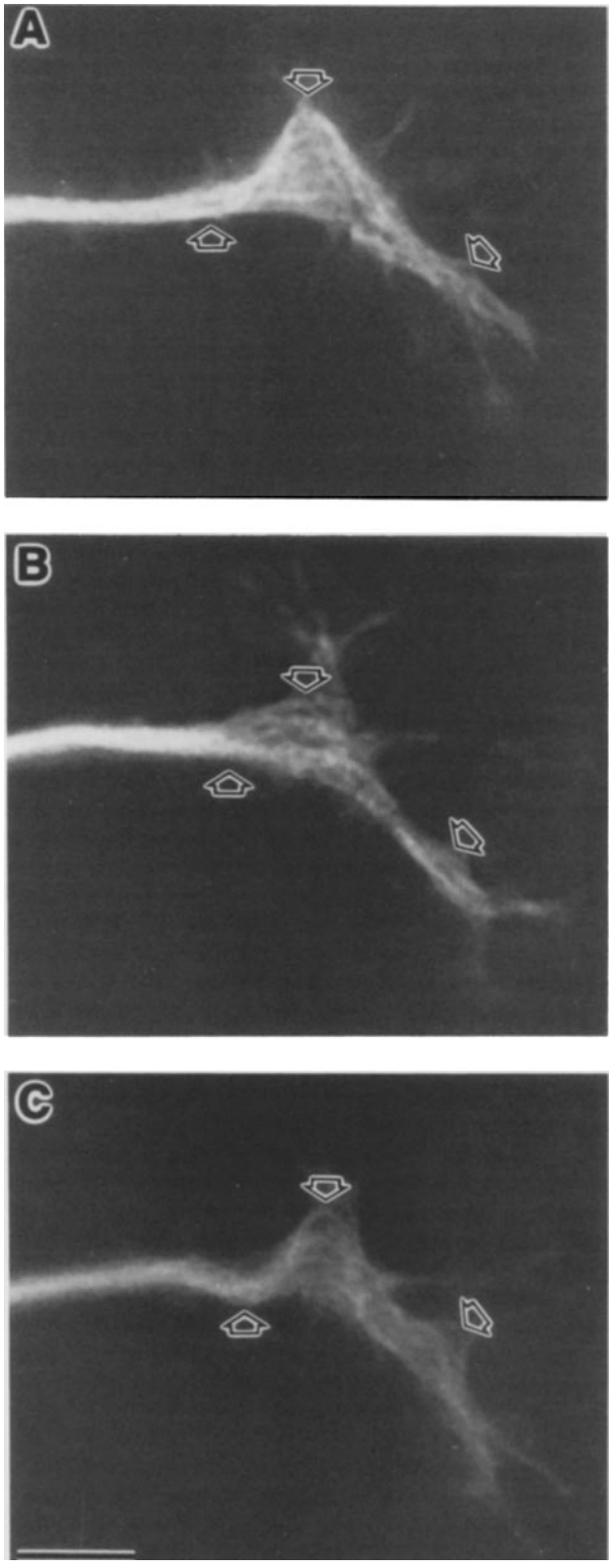

Figure 4. Transient microtubule loop formation in growth cones. This time-lapse sequence of a growth cone in the femur shows the transient formation (*A*), collapse (*B*), and re-formation (*C*) of microtubule loops (*unfilled arrows*). Time *A*, 0 min; *B*, 52 min; *C*, 86 min. Bar, 5 μm.

in Fig. 3 *C* harbored microtubules (low intensity and lack of uniform caliber indicate that the faint signal in the filopodia in Fig. 3 *D* represents background fluorescence).

Branches. In all growth cones, branches were observed. As mentioned above, we operationally defined branches as any elongate protrusion larger in caliber than a filopodium. They usually had a tapering profile so that the base width was greater than the apex width. Unlike filopodia, branches often harbored microtubules. We examined the number of microtubule-invaded branches in growth cones simultaneously labeled with DiO and rhodamine-tubulin. In six growth cones so examined, microtubules were present in 57% of branches (range 40–100%). This is illustrated in Fig. 3 (*A* and *C*), where unfilled arrows indicate branches seen by DiO labeling. The microtubules in those branches can be seen in Fig. 3 (*B* and *D*), respectively. The black arrows in Fig. 3 (*A* and *B*) indicate a branch identified by DiO staining (Fig. 3 *A*), which does not contain microtubules (Fig. 3 *B*). In two cases, short branches were seen to form long before the microtubules selectively invaded the structure (41 and 185 min). This implies that the formation and maintenance of some short branches does not require nearby microtubules, and that branch existence does not imply inevitable microtubule invasion. Indeed, selective and non-random branch invasion seems to be a mechanism used by growth cones to steer at given pathway decisions (see below).

Microtubules Form Complex Loops in the Growth Cone. In 14 growth cones, microtubules were found in complex loop structures. This was usually seen as the growth cone was migrating proximally in the femur (Fig. 1, *box 1*), or was encountering the trochanter-coxa segment boundary (Fig. 1, *box 2*). An example of the former is shown in Fig. 3 (*A* and *B*). The white arrow in Fig. 3 *B* indicates the apex of a group of microtubule loops. The corresponding membrane image, illustrated in Fig. 3 *A*, shows that these loops form within the confines of a smooth growth cone; their presence is not apparent in the shape of the cell itself. Another example of microtubule loops can be seen in Fig. 3 *E*. Here, the microtubules are indicated by the unfilled arrow, and can be seen to loop just under the distal surface of the growth cone. Fig. 3 *F* is an image of the same growth cone shown in Fig. 3 *E*, 34 min later. The microtubule loops can still be seen, and the microtubules indicated by the unfilled arrow have invaded a branch. In many instances, the loops were found to be transient. This is illustrated in Fig. 4, which shows a temporal sequence of images of the same growth cone. The microtubule loops are indicated by the unfilled arrows. They exist in Fig. 4 *A*, collapse in Fig. 4 *B*, and then reform in Fig. 4 *C*.

EM Confirms Microtubule Arrangements. To examine microtubule arrangements and loops at the ultrastructural level, growth cones were imaged, and then prepared for EM. This allowed the correlation of microtubule organization in the imaging study with an electron microscopic analysis of the same growth cone. The growth cone shown in Fig. 3 *F* was fixed shortly after this image was taken, and examined by EM (Fig. 5). The surface of the growth cone is immunolabeled with gold particles (see Methods and Materials). The two branches seen in Fig. 3 *F* can be seen in the upper right and lower left regions of the micrograph. The microtubules indicated by the unfilled arrow in Fig. 3 *F* correspond in configuration and location to those indicated by the large ar-

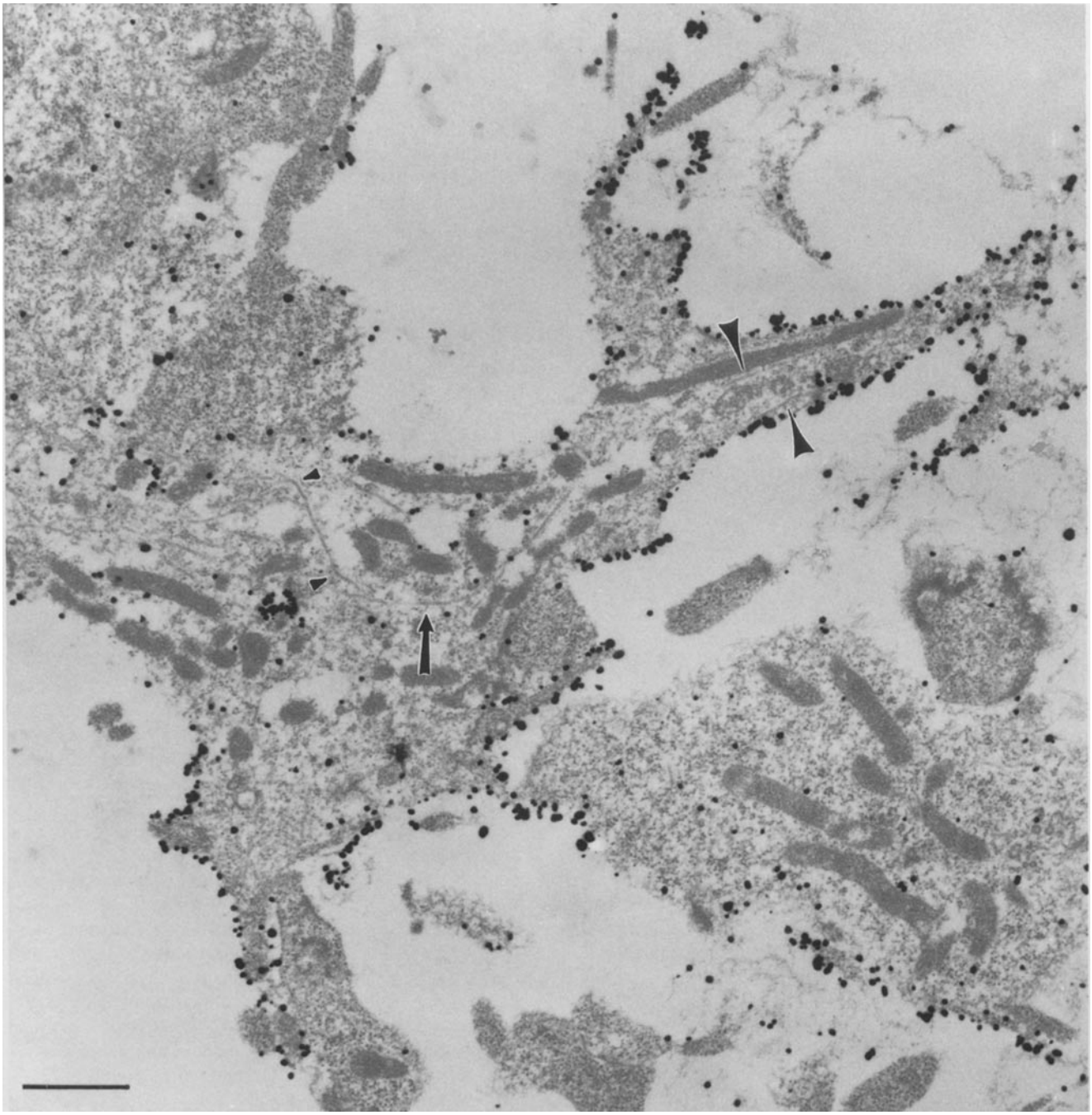

Figure 5. Electron micrograph of a growth cone growing in the femur. The growth cone shown in Fig. 3 *F* was prepared for EM to confirm the arrangement of microtubules seen in the imaging study. The Til growth cone was identified by immunogold visualization of a neuron-specific primary antibody. The curved microtubules seen in Fig. 3 *F* are located in the center of the growth cone (*arrow*). Several individual microtubules can be seen in the dorsal branch (*large arrowheads*). The microtubule indicated by the small arrowheads is shown in detail in Fig. 6. Bar, 1 μm.

rowheads in Fig. 5. Note that they are found as single microtubules. Looped microtubules were also found at the electron microscopic level, and are indicated by the arrow. Fig. 6 shows a higher power image of the same growth cone as in Fig. 5. Looped microtubules, indicated by the small arrowheads in Fig. 5 are indicated by the large arrowheads in Fig. 6. Although the looped microtubule was not continuous at the EM level, it did show bends with similar curvature to that in the fluorescent images. Given that each section was 0.1 μm in thickness, it was not clear whether the looped microtubule was continuous in serial sections.

The Dynamics of Microtubule Movement during Steering Events

Pioneer growth cone steering behavior differs in different limb regions, depending upon the nature of the substrate with which the growth cone is in contact. Several general classes of steering behaviors, including veil extension or

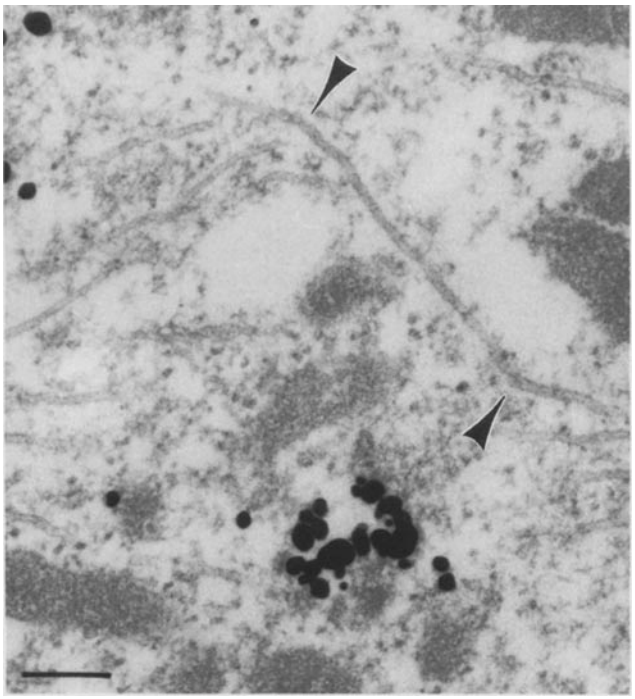

Figure 6. Electron micrograph showing detail of microtubule bending. A higher magnification of the micrograph shown in Fig. 5 illustrating the curvature of microtubules seen in the fluorescent images shown in Fig. 3 *F*. Bar, 1 μm.

retraction, branch extension or retraction and filopodial dilation have been distinguished (O'Connor et al., 1990). We examined microtubule behavior at various limb locations where these three main types of steering events occur.

First, on intrasegmental epithelial cells in the mid-femur region (Fig. 1, *box 1*), the growth cone constantly makes small course corrections to keep it growing proximally along the limb axis (O'Connor et al., 1990). Five growth cones were imaged in this region. The major morphologic form of growth cone migration was by veil extension; initial veil extrusion between filopodia was followed by engorgement of the veil by growth cone cytoplasm. This type of growth is similar to that of PC12 cells and *Aplysia* neurons imaged in vitro (Aletta and Greene, 1988; Goldberg and Burmeister, 1986). Branches were normally present in growth cones in this region, and they often harbored microtubules. Fig. 3 (*A* and *B*) shows a growth cone in the femur, and the branches containing microtubules are indicated by the unfilled arrows. A single branch without microtubules is shown by the black arrow. Usually more than one branch harbored microtubules, although only one was oriented in the future direction of growth cone extension. In this situation, microtubules invaded more than one branch, but were retained in only one. For instance, the growth cone shown in Fig. 3 *F* was in the femur, and microtubules were present in both the dorsal branch, indicated by the unfilled arrow, and the ventral branch, seen in the lower right of the image. Although both branches were generally oriented proximally, that is to the right, the ventral branch was eventually withdrawn and the growth cone extended along the dorsal branch (data not shown). Hence, in this region of the limb, asymmetric microtubule arrangements were set up by selective retention of microtubules in specific branches.

Another type of steering event occurs where the Til growth cone encounters the epithelial cells that form the Tr-Cx limb segment boundary (Fig. 1, *box 2*). The epithelial cells at the boundary are known to differ in shape and surface properties from their intrasegmental counterparts (Bastiani et al., 1991; Caudy and Bentley, 1986*a*; Condic and Bentley, 1989*a*). The growth cones encounter an orthogonal interface between a distal band of highly adhesive epithelial cells (shown as a band of filled hexagons in Fig. 1) and an adjacent proximal band of lower-affinity cells (shown as a band of unfilled hexagons in Fig. 1). At this interface, branches are sent in both dorsal (up in all figures) and ventral directions. The relative size of these branches is quite variable and ranges from large dorsal branches and small ventral branches, through symmetric branch size, to large ventral and small dorsal branches. However, regardless of the initial branch size, the growth cone invariably makes a ventral turn along the boundary.

Five growth cones were imaged as they made this ventral turn at the trochanter-coxa segment boundary. All five represented situations where branches were sent both dorsally and ventrally. Two classes of microtubule movements were seen. In the first class (three cases), microtubules initially invaded both the dorsal and ventral branches. This is illustrated in Fig. 2, which shows a growth cone spreading at the Tr-Cx boundary (the location of the Trl guidepost cell is indicated by the asterisk). Note that the ventral (lower) and dorsal branches, indicated by the white arrows, both contain microtubules, even though the growth cone will eventually turn ventrally. With time, more microtubules were seen to invade the ventral branch (data not shown). In all cases, the dorsal branch and its microtubules persisted during this period. Other studies have shown that this dorsal branch is eventually resorbed (Caudy and Bentley, 1986*b*; O'Connor et al., 1990). This turning mechanism did not seem to involve selective branch invasion by microtubules, but rather selective retention of those microtubules in the ventral branch.

In contrast, the second class (two cases) of microtubule movements at this segment boundary turn did involve selective ventral branch invasion, and is portrayed in Fig. 7. This figure shows a series of images of the same growth cone as it makes the ventral turn at the Tr-Cx segment boundary. The stage was moved slightly after the image in Fig. 7 *C* to follow the growth cone. The growth cone has migrated to the Trl cell, which is indicated by the black arrow in Fig. 7 *A*. At this point, several filopodia and small branches extend both dorsally and ventrally along the segment boundary, at the right of each of the panels. The microtubules form a closely packed bundle in the growth cone in Fig. 7 *C*, but are not oriented dorsoventrally along the boundary. In Fig. 7 *D*, however, the bundle shows a slight ventral orientation. Note that no microtubules have entered the dorsal or proximal branches seen in the upper right region of Fig. 7 *D*. The ventral branch, which is also void of microtubules at this time, is shown by the arrowheads in Fig. 7 *D*. In Fig. 7 *E*, the microtubules have clearly entered the ventral branch (indicated by the *arrowheads*). The dorsal branches persisted for the duration of the imaging, but they never harbored microtubules. No morphologic differences were apparent between growth cones that used this type of turning and those in the former class. Although these two classes of microtubule movements differed in whether the dorsal branch harbored

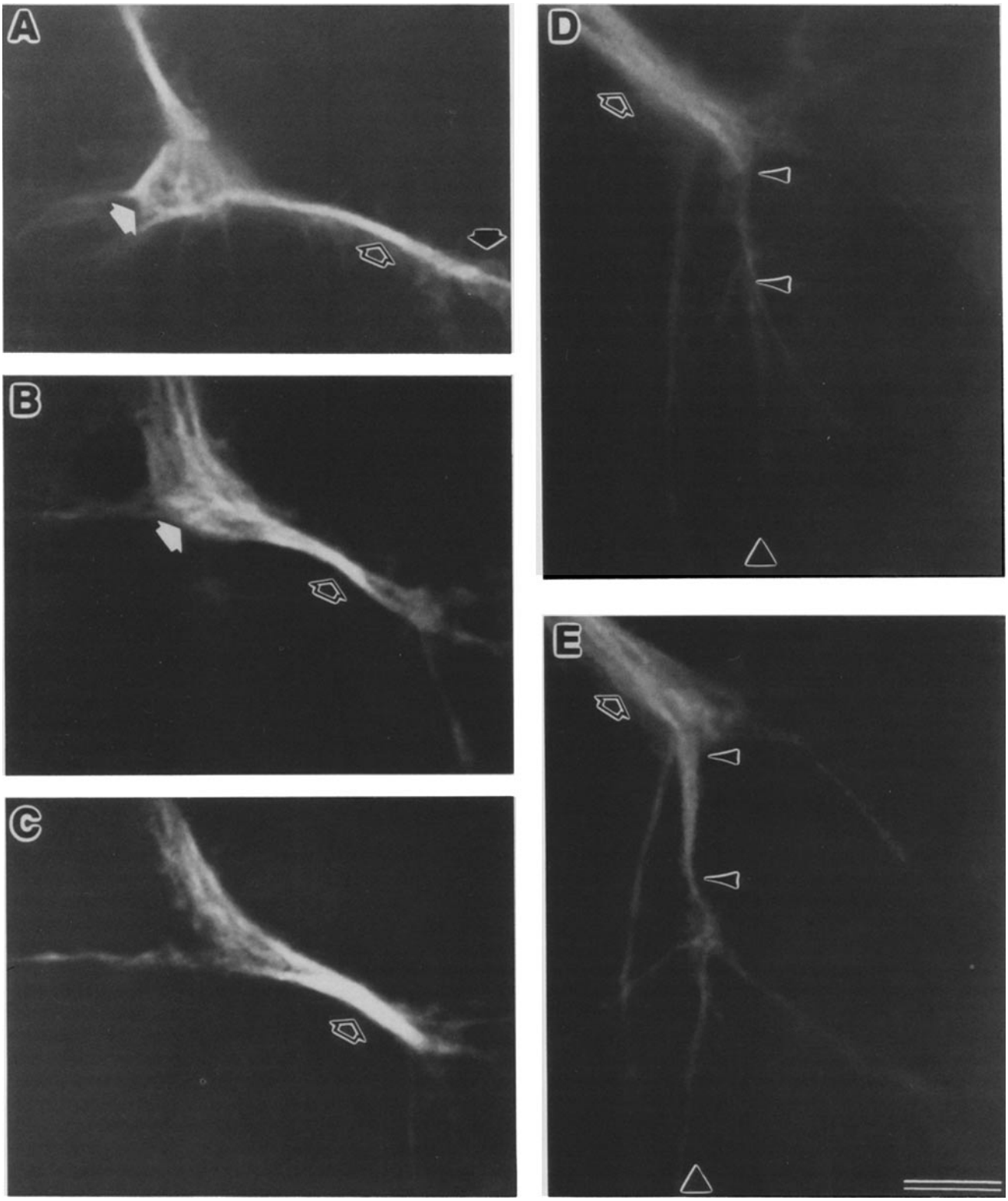

Figure 7. Selective microtubule invasion during a growth cone steering event at a limb segment boundary. (*A*) Time, 0 min. The position of this rhodamine-tubulin–labeled pioneer neuron growth cone is shown in Fig. 1 (*box 2*). A pronounced microtubule loop is present at the Fe-Tr segment boundary (*white arrow*). A small bundle of microtubules (*unfilled arrow*) extends along the process which contacts the Trl cell (*black arrow*) located at the Tr-Cx segment boundary. (*B*) Time, 2 h, 31 min. The process extending to the Tr-Cx boundary has thickened (*unfilled arrow*). The loop at the Fe-Tr boundary (*white arrow*) has straightened, and the axon distal to this boundary (that is, left of the *white arrow*) has enlarged. (*C*) Time, 2 h, 56 min. The process extending to the Tr-Cx boundary continues to enlarge (*unfilled arrow*). (*D*) Time, 4 h, 55 min. The process extending to the Tr-Cx boundary has expanded to normal axonal caliber (*unfilled arrow*). The Tr-Cx segment boundary is indicated by the triangle. Microtubules end abruptly at the boundary, although filopodia and branches have extended in several directions including ventrally (*arrowheads*). (*E*) Time, 7 h, 9 min. Microtubules (*arrowheads*) have selectively invaded the branches extending ventrally, in the direction the growth cone will take. Microtubules did not invade branches extended dorsally or proximally. Bar, 5 μm.

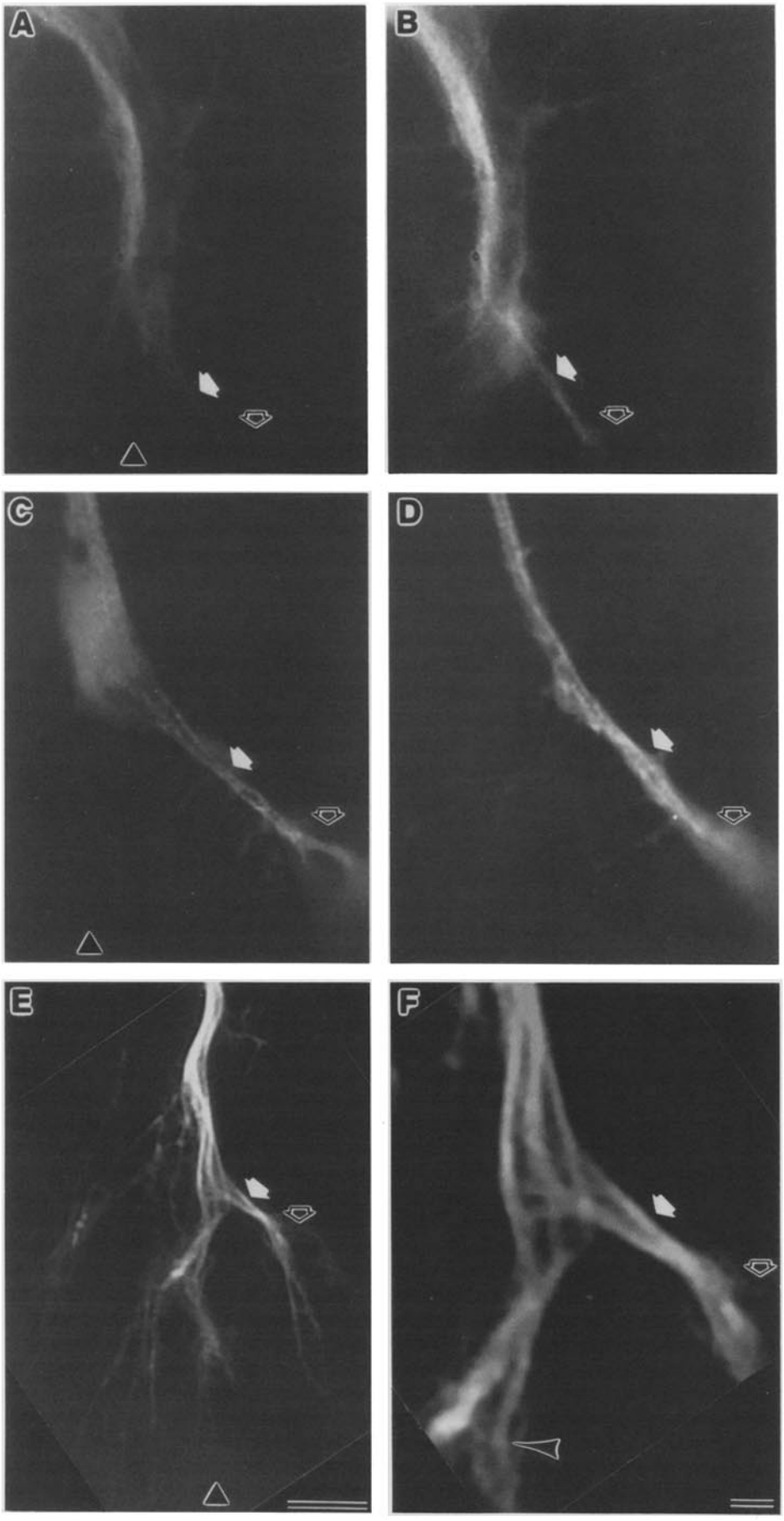

Figure 8. Selective microtubule invasion during growth cone steering events at the Cx1 guidepost cells. Three rhodamine-tubulin–labeled growth cones (*A–B*, *C–D*, and *E–F*) are imaged as they reorient abruptly at the Cx1 guidepost cells (Fig. 1, *box 3*). (*A*) Time, 0 min. A growth cone migrating ventrally along the Tr-Cx segment boundary (shown by *triangle*) extends a single filopodium (*white arrow*) to contact the Cx1 cells (*unfilled arrow*). (*B*) Time, 28 min. The filopodium now has a branch morphology, and has been invaded by microtubule(s) (*white arrow*). Microtubules have not invaded other regions of the growth cone. (*C*) Time, 0 min. Another growth cone at a slightly later stage has a broad lamellum on the Tr-Cx segment boundary (indicated by the *triangle*). A small number of microtubules (*white arrow*) are present in the process crossing from the segment boundary to the Cx1 cells (*unfilled arrow*). (*D*) Time, 51 min. The lamellum has withdrawn from the boundary, and the nascent axon (*white arrow*) crosses from the boundary to the Cx1 cell (*unfilled arrow*). (*E*) Another growth cone, extending ventrally along the Tr-Cx boundary (*triangle*), also has a process (*white arrow*) extending across the boundary to the Cx1 cells (*unfilled arrow*). (*F*) In an enlarged view of the branch point shown in *E*, it appears that microtubules diverge from three different microtubule bundles present along the Tr-Cx boundary to enter the branch (*white arrow*) crossing to the Cx1 cells (*unfilled arrow*). Some microtubules (*arrowhead*) continue along the boundary past the branch point. In such cases, the growth cone may have advanced along the boundary past the Cx1 cells before the first filopodial contact with those cells. Bars: (*A–E*) 5 μm; (*F*) 1 μm.

microtubules, both turns eventually involved the streaming of microtubules into the ventral branch. Hence, at the steering decision made at the Tr-Cx segment boundary, both selective invasion and selective retention were seen as mechanisms of generating asymmetric microtubule arrangements.

The third, and perhaps most striking, of the steering mechanisms used by the Til pioneer neurons is elicited by an interaction between the Til growth cone and guidepost cells. Three guidepost cells are found in the Til pathway: Fel, Trl, and the Cxl pair. A major growth cone reorientation occurs at the Cxl turn (shown in Fig. 1, *box 3*). This turn was imaged three times, and the smaller angle Trl turn was imaged twice. In all five cases, the turns were accomplished by selective invasion of a single growth cone branch by microtubules. Fig. 8 (*A* and *B*) shows a growth cone making the turn to the Cxls. The growth cone has migrated ventrally along the segment boundary, which is indicated by the triangle in Fig. 8 *A*. The location of the Cxl cells is indicated by the unfilled arrow. In Fig. 8 (*A* and *B*), note that filopodia and branches extend from the growth cone in both proximal (to the right) and distal (to the left) directions. A single filopodium can be seen extending to the Cxls, as shown by the white arrow. Fig. 8 *B* shows the same growth cone 28 min later; microtubule(s) have selectively invaded the branch which has formed from the filopodium extending to the Cxl cells (Fig. 8, *white arrow*). Therefore, microtubules had selectively extended in the direction of growth cone migration. This selectivity occurred when there was only one branch present, extending to the Cxl cells, and also when additional proximal or distal branches were present as in Fig. 8 (*A* and *B*). Fig. 8 (*C* and *D*) shows another growth cone at a later stage in the turn. The initially small number of microtubules that have entered the branch extending to the guidepost cell have become the nascent axon microtubule fascicle as the turn is completed.

Previous studies of this turn indicate that occasionally a proximally extended filopodium may not make contact with a Cxl cell until after the leading edge of the growth cone has migrated ventrally past the cell (Caudy and Bentley, 1986*b*; O'Connor et al., 1990). We imaged one growth cone where this pattern of growth apparently occurred. In this situation, the branch contacting the Cxl guidepost cell harbored microtubules that appeared to originate directly from the main growth cone bundles. This is shown in Fig. 8 *E*, and in higher magnification in Fig. 8 *F*. The location of the Cxl cells is indicated by the unfilled arrow, and the triangle in Fig. 8 *E* shows the location of the Tr-Cx segment boundary. Note that four microtubule bundles seem to arise from larger bundles within the growth cone, and enter the branch extending to the Cxl cell (Fig. 8, *white arrow*). The arrowhead in Fig. 8 *F* shows microtubules in the distal region of the growth cone, which had migrated past the Cxl cells.

Before growth cones make the turn at the trochanter-coxa boundary (Fig. 1, *box 2*), a guidepost cell mediated turn occurs at the Trl cell. A single filopodial contact with the Trl guidepost cell serves to reorient the growth cone by filopodial dilation. We observed two growth cones at this location where a small number of microtubules selectively entered a branch in contact with the Trl cell. The later stages of one such turn is shown in the first three panels of Fig. 7. The Trl guidepost cell is indicated by the black arrow, and the branch contacting it by the unfilled arrow. Although other filopodia and small branches were present, microtubules only entered the branch extending to Trl. Subsequently, additional microtubules accrued within this branch until it reached the caliber of the nascent axon (Fig. 7 *D*). These results suggest that at all guidepost cells, steering by selective filopodial dilation is accompanied by selective microtubule invasion.

Discussion

In the embryonic grasshopper leg, the migration of the Til pioneer growth cones follows a stereotyped pathway (Fig. 1) from the tibia to the central nervous system, a path length of ~0.5 mm (Bate, 1976; Bentley and Caudy, 1983; Caudy and Bentley, 1986*b*; Ho and Goodman, 1982). Guidance over this complex pathway is accomplished by many growth cone-cell interactions including those involving intrasegmental epithelial cells, segment boundary epithelial cells, and preaxonogenesis neurons called guidepost cells (Caudy and Bentley, 1986*b*; Condic and Bentley, 1989*b*; Keshishian and Bentley, 1983; Lefcort and Bentley, 1987; O'Connor et al., 1990). Guidance features which mediate normal growth cone migration are preserved in a limb fillet preparation where individual cells are accessible for observation and experimental manipulation (Lefcort and Bentley, 1987; O'Connor et al., 1990). We observed microtubule arrangements during growth cone migration in response to these in situ guidance cues by injecting the Til neuron with rhodamine-labeled tubulin.

Labeled bovine tubulin rapidly incorporated into linear tracks in the axon and growth cone. This is consistent with the high degree of homology between bovine and insect tubulin (Rudolph et al., 1987). Projection of the image onto a high resolution CCD chip, deconvolution of multiple image planes, and use of conventional computer image enhancement software provided adequate resolution of linear tracks. Individual tracks were uniform in width and intensity along their whole length. Furthermore, within the same growth cone, different tracks were uniform in width and intensity. Widths corresponded closely to those reported for fluorescently labeled microtubules whose unity and identity were subsequently confirmed in electron micrographs (Sammak and Borisy, 1988). Electron micrographs of Til growth cones fixed immediately after imaging revealed individual microtubules similar in location and shape to fluorescent tracks previously imaged in the same growth cone (Figs. 5 and 6, *arrowheads*). These results strongly suggest that the unitary fluorescent tracks were individual microtubules. These are the first observations of individual microtubule disposition and behavior in growth cones migrating and steering on the in situ substrate.

The Arrangement of Microtubules in Til Neurons

Axons. In both fixed and live neurons in vitro, microtubules in the axon are arranged in a closely packed, linear bundle (Black et al., 1989; Brady et al., 1984; Bray and Hollenbeck, 1988; Heidemann et al., 1984; Hirokawa et al., 1988; Keith, 1990; Meininger and Binet, 1989). This arrangement was also seen in Til axons in situ (see Figs. 3 *F* and 4). Although axonal microtubules were generally in this configuration, occasionally they could be displaced to one side or splay out into small bundles, especially at the locations of lateral protrusions.

In neurons viewed in vitro, the border between the growth

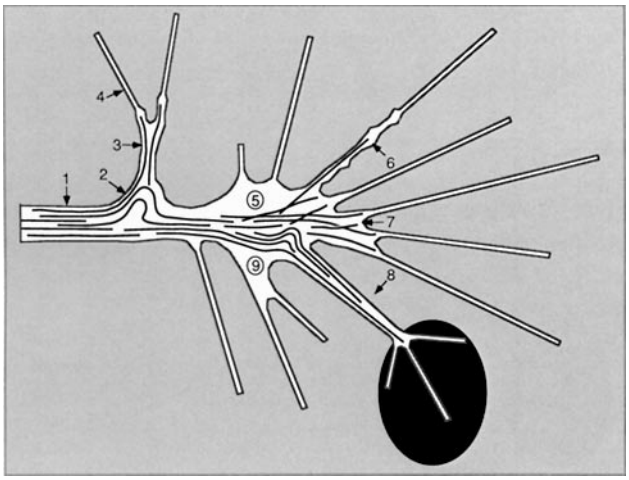

Figure 9. A diagram of features of microtubule arrangements in pioneer growth cones in situ. (*1*) Bundled microtubules in the axon. (*2*) Microtubule loops seen at axonal branch points and in the growth cone. (*3*) Bundles of microtubules extending into a branch. (*4*) Absence of microtubules in filopodia. (*5*) Regions of the growth cone periphery can be devoid of microtubules. (*6*) Where a filopodium expands into a branch, microtubule invasion is often observed. (*7*) Microtubules often extend to the growth cone periphery. (*8*) Microtubules selectively invade a branch formed from a filopodium which has contacted a guidepost cell. (*9*) Some branches are devoid of microtubules.

cone and axon is defined as that region where the axonal cylinder abruptly increases in caliber (Bray and Chapman, 1985; Goldberg and Burmeister, 1986). At this border there is a transition in the arrangement of both actin and microtubules (Forscher and Smith, 1988; Mitchison and Kirschner, 1988). In this region, the microtubule arrangement changes from the highly bundled form in the axon to the splayed out pattern in the growth cone. In some Til neurons, this change was easily identifiable. Furthermore, the location of the change in microtubule arrangement could be displaced from the change in cell shape at the border between the growth cone and axon (Fig. 3 *F*). It would seem that the formation of the closely packed bundle of microtubules characteristic of the axon can occur centrally within the growth cone. This suggests that the formation of an axon may first involve the formation of a tight bundle of microtubules in the growth cone, and subsequently the collapse of the plasma membrane around that bundle. This process has been seen in live *Xenopus* neurons viewed in time lapse in vitro (Tanaka and Kirschner, 1991). It is likely that the axonal bundling in the growth cone reflects the activity of microtubule associated proteins (Matus, 1990), suggesting that the activity of such molecules is spatially localized to the axon and central growth cone.

Growth Cones. The grasshopper Til growth cones in situ have a rich investment of microtubules. This and other features of the Til growth cone are shown in schematic form in Fig. 9. An issue on which previous observations have varied is the degree to which microtubules are confined to the central core area of the growth cone. In some early electron microscope studies (Bunge, 1973; Isenberg and Small, 1978), and in live *Aplysia* bag cell growth cones which are immobilized on a highly adhesive substrate (Forscher and Smith, 1988), microtubules rarely extend to the growth cone margin. In other studies, on fixed and extracted chick sensory and retinal neuron, or rat sympathetic growth cones (Bridgman and Dailey, 1989; Letourneau, 1983; Letourneau and Shattuck, 1989; Tsui et al., 1984), and live *Xenopus* growth cones in vitro (Tanaka and Kirschner, 1991), microtubules regularly extend to the distal margin of the growth cone. In Til neurons in situ, the usual situation is for a dense array of microtubules to be extended right up to the leading margin of the growth cone (Fig. 2). Thus, the distal growth cone region of Til pioneer neurons appears to be more heavily invested with microtubules than has been observed in some growth cones in vitro.

Filopodia extending from Til growth cones in situ never harbored microtubules (Figs. 3, *C* and *D* and 9). These in situ observations are in accordance with previous in vitro studies, at both the light and electron microscope levels, indicating that filopodia are composed primarily of F-actin and lack microtubules (Bridgman and Dailey, 1989; Letourneau, 1983; Smith, 1988). In neurons in vitro, and in Til neurons in vivo, cytochalasin-induced disassembly of filamentous actin results in the loss of filopodia, suggesting that actin is necessary for filopodial extension and maintenance (Bentley and Toroian-Raymond, 1986; Marsh and Letourneau, 1984).

Unlike filopodia, branches extending from the Til growth cone often did harbor microtubules (Figs. 2 and 9). However, approximately half of the growth cone branches did not contain microtubules (see Fig. 3, *A* and *B*). This is in accordance with observations of fixed neurons in vitro, where branches both with and without microtubules have been observed (Tsui et al., 1984). Furthermore, many short branches formed and existed without nearby microtubules. We conclude that microtubules are not necessary for the initiation of branch formation, nor for the maintenance of short branches.

Branches can be formed from preexisting filopodia. This is perhaps best appreciated in those branches that form from filopodia in contact with guidepost cells. After the filopodium contacts a guidepost cell, it increases in caliber and eventually converts to a branch (O'Connor et al., 1990). Such branches always acquired microtubules. However, the conversion of the filopodium to a branch always occurred in advance of the acquisition of microtubules. In Fig. 8 *A*, for example, a filopodium contacted the Cx1 guidepost cells. However, microtubules did not invade the structure until it has undergone a conversion to a branch some 30 min later (Fig. 8 *B*). Thus, filopodia did not appear to be enlarged by the process of microtubule intrusion; rather, microtubules always intruded into a space that was already present.

Microtubule Movement during Steering Events

The finding that many microtubules are normally present in the growth cone and in branches of Til growth cones in situ raises the possibility that they may play a direct role in certain phases of steering. The process of growth cone steering can be formally divided into three phases. The first phase comprises exploration or sampling of the environment in the vicinity of the growth cone. It appears to be mediated by the random protrusion of filopodia; there is no evidence that filopodial extension is preferentially directed towards the target. Before a turn is made, however, one or a few of the branches or filopodia must be chosen as the future track of

the extending growth cone. This second phase of steering is called orientation. The cytoskeletal requirements for orientation are not known. The final phase of steering is consolidation and conversion of the arrangements of cytoskeletal and other molecular features of the growth cone to the chemically and mechanically more stable configurations found in the nascent axon.

While the absence of microtubules from filopodia indicates that microtubules are unlikely to be important in the exploration phase, their disposition appears to be a key element of the orientation phase. This can be seen in Fig. 8 (*A* and *B*). At the beginning of this phase (Fig. 8 *A*), their disposition is not oriented, and at its end (Fig. 8 *B*) their placement defines where consolidation into the nascent axon can occur. Consolidation is shown in Fig. 8 (*C* and *D*). Hence, we suggest that the endpoint of orientation is the generation of an asymmetric arrangement of microtubules in the growth cone. There are two general mechanisms by which this can be accomplished. One is that microtubules could invade only those branches that are found in the future direction of growth cone extension. We term this selective microtubule invasion. An alternative mechanism would be that microtubules randomly invade all extant branches, and are subsequently stabilized in those extending in the preferred direction. This we term selective microtubule retention. The microtubule imaging in this study allows one to address directly which mechanism is operating at a given turn.

At guidepost cell induced turns, such as those at Tr1 and Cx1, selective microtubule invasion was seen invariably (Figs. 8 and 9). In addition, this selective mechanism was also seen in two of five turns observed at the trochanter-coxa segment boundary (Fig. 7). In contrast to this, three of five turns at the segment boundary were made using selective retention to generate an asymmetric microtubule arrangement; microtubules invade both the ventral and dorsal branches (Fig. 2). Intrusion of microtubules into some, but not all branches was also seen in growth cones migrating proximally through the femur (Fig. 3). Therefore, both selective microtubule invasion and selective microtubule retention appear to underlie steering decisions, depending on the growth cone location in the limb.

The mechanism used to generate the asymmetric microtubule arrangement is likely to be determined by both the heterogeneity and nature of guidance information confronted by the growth cone during the exploratory phase (O'Connor et al., 1990). At guidepost cell-mediated turns, the observed selective microtubule invasion may reflect a large difference in the signal provided by a single, highly localized, high affinity, guidepost cell, and the surrounding cells. Selective microtubule retention, on the other hand, may occur where the differences between the substrates encountered by Til filopodia are not so dissimilar. Both at different locations within the femur, and along the segment boundary, the spatial rate of change of substrate affinity may be quite low. In this more ambiguous situation, the sequence from filopodial contact with an acceptable substrate, to branch formation, to accrual of successive microtubules into the branch, to consolidation of a large bundle of microtubules may proceed through several steps before one branch prevails. Thus selective microtubule invasion of a single branch and selective microtubule retention following multi-branch invasion seem likely to be extremes of a range of microtubule behavior which is dependent upon the disparity between environment-dependent intracellular signals in different growth cone regions.

What sort of signals may be involved? The generation of heterogeneous microtubule arrangements is central to many cellular processes, including yeast bud formation (Adams and Pringle, 1984), pigment granule aggregation in teleost retina (Troutt and Burnside, 1988), epithelial cell response to wounds, and spindle formation during mitosis (Kirschner and Mitchison, 1986; Mitchison and Kirschner, 1985). Of these, the mechanism by which the microtubules are arranged has been investigated in the most detail in spindle formation. Here, it appears that during formation of the spindle, microtubules randomly assemble, and are selectively stabilized by contact with the kinetochore (Cassimeris et al., 1990; Hayden et al., 1990; Mitchison et al., 1986). A similar situation could underlie selective retention of microtubules in selected growth cone regions or branches.

Where selective invasion occurs, it seems likely that certain regions of the growth cone are more receptive to microtubule invasion or assembly. The molecular and biophysical basis for selective microtubule invasion is unknown. It appears that under baseline conditions, microtubule invasion may be prevented by the physical presence of the peripheral actin network. This is suggested by ultrastructural observations (Letourneau, 1983), experimental perturbations of actin in growth cones in vitro (Forscher and Smith, 1988; Smith, 1988), and by biophysical considerations of diffusion coefficients in actin gels (Luby-Phelps et al., 1988). If this is the case, then contact with high affinity cues must locally alter this situation. This alteration could be effected by spatially restricted changes in tension (Bray and Hollenbeck, 1988; Heidemann et al., 1990; Letourneau, 1975), and/or the concentration of second messengers molecules (Bentley et al., 1991; Bixby, 1989; Forscher, 1989; Kater and Mills, 1991; Lankford and Letourneau, 1989; Letourneau and Shattuck, 1989). It is also possible that these effector molecules change a chemical interaction between actin and microtubules that promotes microtubule invasion (Goslin et al., 1989; Letourneau, 1983; Morales and Fifkova, 1989).

Another issue raised by our findings is the nature of the mechanism by which microtubules invade growth cone branches. This invasion may represent new microtubule assembly from the monomeric tubulin pool onto the distal, plus ends of the microtubules (Baas and Black, 1990; Bamburg et al., 1986). Alternatively, microtubules could be translocated into branches. One approach to distinguishing these alternatives would be to make a small fluorescent mark on the microtubules, and then observe the movement of the mark as microtubules invade the growth cone. This type of study has been carried out; it was found that microtubules marked in the axon near the growth cone move distally into the growth cone, even in the absence of axonal elongation (Reinsch et al., 1991). This suggests that microtubule translocation may contribute to branch invasion.

One of the most striking features of the Til growth cones in situ was the regular occurrence of transient microtubule loops. Looping microtubules have been described before in fixed, permeabilized growth cones in vitro (Lankford and Klein, 1990; Tsui et al., 1984). They have also been seen to form and collapse in real time imaging of live *Xenopus* neurons in vitro (Tanaka and Kirschner, 1991). Their presence

in time-lapse images of migrating Til growth cones, subsequently confirmed by electron microscopy, indicates that they are normal features in process outgrowth. Although microtubule polymers have been described as biophysically rigid when compared to other cytoskeletal polymers (Mizushima-Sugano et al., 1983), the forces required to bend microtubules could be supplied by the GTP hydrolysis associated with assembly, or by the ATP hydrolysis associated with microtubule based motors (Hill, 1987). Whatever the source, this force could provide the energy needed to allow microtubules to invade selective regions of the growth cone.

A schematic showing the major types of microtubule arrangements found in the Til pioneer growth cone in situ is shown in Fig. 9. Many of these features may contribute to strategies underlying growth cone steering. Further studies on the molecular nature of microtubule stabilization and interaction with other cytoskeletal and second messenger elements in the growth cone will increase our understanding of how neurons steer toward their target, and generate the connections of the adult nervous system.

We thank E. Tanaka, S. Reinsch, and F. Lefcort for stimulating comments on the experiments; T. Mitchison, R. Vale, and K. Lankford for comments on the manuscript; and L. Reichardt for allowing use of his imaging system. Support for this work was provided by Medical Research Council of Canada fellowships to J. H. Sabry and T. P. O'Connor, National Science Foundation Biological Facilities Center Grant BBS-8714246 to the University of California at Berkeley, Lucille Markey Foundation Award to the University of California at San Francisco Imaging Center, National Institutes of Health Javits Award NS09074-22 to D. Bentley and a National Institute of General Medical Sciences grant to M. W. Kirschner.

Received for publication 17 May 1991 and in revised form 24 June 1991.

References

Adams, A. E. M., and J. R. Pringle. 1984. Relationship of actin and tubulin distribution in wild-type and morphogenetic mutant *Saccharomyces cerevisiae*. *J. Cell Biol.* 98:934–945.

Aletta, J. M., and L. A. Greene. 1988. Growth cone configuration and advance: a time-lapse study using video-enhanced differential interference contrast microscopy. *J. Neurosci.* 8:1425–1435.

Anderson, H. 1988. *Drosophila* adhesion molecules and neural development. *Trends Neurosci.* 11:472–475.

Anderson, H., and R. P. Tucker. 1988. Pioneer neurons use basal lamina as a substratum for outgrowth in the embryonic grasshopper limb. *Development (Camb.)* 104:601–608.

Baas, P. W., and M. M. Black. 1990. Individual microtubules in the axon consist of domains that differ in both composition and stability. *J. Cell Biol.* 111:495–509.

Bamburg, J. R., D. Bray, and K. Chapman. 1986. Assembly of microtubules at the tip of growing axons. *Nature (Lond.).* 321:778–790.

Bastiani, M. J., H. G. deCouet, J. M. A. Quinn, K. J. Kotrla, K. J. Karlstrom, C. S. Goodman, and E. E. Ball. 1991. Transient and dynamic expression of meg protein during development of the grasshopper embryo. *Dev. Biol.* In press.

Bate, C. M. 1976. Pioneer neurones in an insect embryo. *Nature (Lond.).* 260:54–56.

Bentley, D., and M. Caudy. 1983. Navigational substrates for peripheral pioneer growth cones: limb-segment boundaries, and guidepost neurons. *Cold Spring Harbor Symp. Quant. Biol.* 48:573–585.

Bentley, D., and H. Keshishian. 1982. Pathfinding by peripheral pioneer neurons in grasshoppers. *Science (Wash. DC).* 218:1082–1088.

Bentley, D., and A. Toroian-Raymond. 1986. Disoriented pathfinding by pioneer neurone growth cones deprived of filopodia by cytochalasin treatment. *Nature.* 323:712–715.

Bentley, D., P. B. Guthrie, and S. B. Kater. 1991. Calcium ion distribution in nascent pioneer axons and coupled preaxonogenesis neurons in situ. *J. Neurosci.* 11:1300–1308.

Bixby, J. L. 1989. Protein kinase C is involved in laminin stimulation of neurite outgrowth. *Neuron.* 3:287–297.

Black, M. M., P. W. Baas, and S. Humphries. 1989. Dynamics of alpha-tubulin deacetylation in intact neurons. *J. Neurosci.* 9:358–368.

Brady, S. T., M. Tyell, and R. J. Lasek. 1984. Axonal tubulin and axonal microtubules: biochemical evidence for cold-stability. *J. Cell Biol.* 99:1716–1724.

Bray, D., and K. Chapman. 1985. Analysis of microspike movements on the neuronal growth cone. *J. Neurosci.* 5:3204–3213.

Bray, D., and P. J. Hollenbeck. 1988. Growth cone motility and guidance. *Annu. Rev. Cell Biol.* 4:43–61.

Bridgman, P. C., and M. E. Dailey. 1989. The organization of myosin and actin in rapid frozen nerve growth cones. *J. Cell Biol.* 108:95–109.

Bunge, M. B. 1973. Fine structure of nerve fibers and growth cones of isolated sympathetic neurons in culture. *J. Cell Biol.* 56:713–735.

Cassimeris, L., C. L. Rieder, G. Rupp, and E. D. Salmon. 1990. Stability of microtubule attachment to metaphase kinetochores in PtK1 cells. *J. Cell Sci.* 96:9–15.

Castleman, K. R. 1979. Digital Image Processing. Prentice-Hall, Inc., Englewood Cliffs, NJ. 429 pp.

Caudy, M., and D. Bentley. 1986*a*. Epithelial cell specialization at a limb segment boundary in the grasshopper embryo. *Dev. Biol.* 118:399–402.

Caudy, M., and D. Bentley. 1986*b*. Pioneer growth cone steering along a series of neuronal and non-neuronal cues of different affinities. *J. Neurosci.* 6: 1781–1795.

Caudy, M., and D. Bentley. 1987. Pioneer growth cone behavior at a differentiating limb segment boundary in the grasshopper embryo. *Dev. Biol.* 119: 454–465.

Condic, M. L., and D. Bentley. 1989*a*. Pioneer growth cone adhesion in vivo to boundary cells and neurons after enzymatic removal of basal lamina in grasshopper embryos. *J. Neurosci.* 9:2687–2696.

Condic, M. L., and D. Bentley. 1989*b*. Pioneer neuron pathfinding from normal and ectopic locations in vivo after removal of the basal lamina. *Neuron.* 3:427–439.

Dodd, J., and T. M. Jessell. 1988. Axon guidance and the patterning of neuronal projections in vertebrates. *Science (Wash. DC).* 242:692–699.

Elkins, T., M. Hortsch, A. J. Bieber, P. M. Snow, and C. S. Goodman. 1990. Drosophila fasciclin I is a novel homophilic adhesion molecule that along with fasciclin III can mediate cell sorting. *J. Cell Biol.* 110:1825–1832.

Fessler, J. H., and L. I. Fessler. 1989. *Drosophila* extracellular matrix. *Annu. Rev. Cell Biol.* 5:309–339.

Forscher, P. 1989. Calcium and polyphosphoinositide control of cytoskeletal dynamics. *Trends Neurosci.* 12:468–474.

Forscher, P., and S. J. Smith. 1988. Actions of cytochalasins on the organization of actin filaments and microtubules in a neuronal growth cone. *J. Cell Biol.* 107:1505–1516.

Goldberg, D. J., and D. W. Burmeister. 1986. Stages in axon formation: observations of growth of *Aplysia* axons in culture using video-enhanced contrast-differential interference contrast microscopy. *J. Cell Biol.* 103:1921–1931.

Goldberg, D. J., and D. W. Burmeister. 1989. Looking into growth cones. *Trends Neurosci.* 12:503–506.

Goodman, C. S., M. J. Bastiani, D. Q. Doe, S. du Lac, S. L. Helfand, J. Y. Kuwada, and J. B. Thomas. 1984. Cell recognition during neuronal development. *Science (Wash. DC).* 21:1271–1279.

Goslin, K., E. Birgbauer, G. Banker, and F. Solomon. 1989. The role of cytoskeleton in organizing growth cones: a microfilament-associated growth cone component depends upon microtubules for its localization. *J. Cell Biol.* 109:1621–1631.

Harris, W. A., C. E. Holt, and F. Bonhoeffer. 1987. Retinal axons with and without their somata, growing to and arborizing in the tectum of Xenopus embryos: a time-lapse video study of single fibres in vivo. *Development (Camb.).* 101:123–133.

Harrison, R. G. 1910. The outgrowth of the nerve fiber as a mode of protoplasmic movement. *J. Exp. Zool.* 17:521–544.

Hayden, J. H., S. S. Bowser, and C. L. Rieder. 1990. Kinetochores capture astral microtubules during chromosome attachment to the mitotic spindle: direct visualization in live newt lung cells. *J. Cell Biol.* 111:1039–1045.

Heidemann, S. R., M. A. Hamborg, S. J. Thomas, B. Song, S. Lindley, and D. Chu. 1984. Spatial organization of axonal microtubules. *J. Cell Biol.* 99:1289–1295.

Heidemann, S. R., P. Lamoureux, and R. E. Buxbaum. 1990. Growth cone behavior and production of traction force. *J. Cell Biol.* 111:1949–1957.

Hill, T. L. 1987. The macroscopic aggregate as a limiting case. *In* Linear Aggregation Theory in Cell Biology. Hill, T. L., editor. Springer-Verlag, New York. 23–31.

Hiraoka, Y., J. W. Sedat, and D. A. Agard. 1987. The use of a charge-coupled device for quantitative optical microscopy of biological structures. *Science (Wash. DC).* 238:36–41.

Hirokawa, N., S. Hisanaga, and Y. Shiomura. 1988. MAP2 is a component of crossbridges between microtubules and neurofilaments in the neuronal cytoskeleton: quick-freeze, deep-etch immunoelectron microscopy and reconstitution studies. *J. Neurosci.* 8:2769–2779.

Ho, R. K., and C. S. Goodman. 1982. Peripheral pathways are pioneered by an array of central and peripheral neurones in grasshopper embryos. *Nature (Lond.).* 297:404–406.

Hyman, A., D. Drechsel, D. Kellog, S. Salser, K. Sawin, P. Steffen, L. Wordeman, and T. Mitchison. 1991. Preparation of modified tubulins. *Methods Enzymol.* 196:478–485.

Isenberg, G., and J. V. Small. 1978. Filamentous actin, 100-A filaments and microtubules in neuroblastoma cells, their distribution in relation to sites of

movement and neuronal transport. *Eur. J. Cell Biol.* 16:326–344.
Jan, L. Y., and Y. N. Jan. 1982. Antibodies to horseradish peroxidase as specific neuronal markers in *Drosophila* and grasshopper embryos. *Proc. Natl. Acad. Sci. USA.* 79:2700–2704.
Kater, S. B., and L. R. Mills. 1991. Regulation of growth cone behavior by calcium. *J. Neurosci.* 11:891–899.
Keith, C. H. 1990. Neurite elongation is blocked if microtubule polymerization is inhibited in PC12 cells. *Cell Motil. Cytoskeleton.* 17:95–105.
Keshishian, H., and D. Bentley. 1983. Embryogenesis of peripheral nerve pathways in grasshopper legs. *Dev. Biol.* 96:98–124.
Kirschner, M. W., and T. J. Mitchison. 1986. Beyond self-assembly: from microtubules to morphogenesis. *Cell.* 45:329–342.
Lankford, K. L., and W. L. Klein. 1990. Ultrastructure of individual neurons isolated from avian retina: occurrence of microtubule loops in dendrites. *Brain Res. Dev. Brain Res.* 51:217–224.
Lankford, K.L., and P. C. Letourneau. 1989. Evidence that calcium may control neurite outgrowth by regulating the stability of actin filaments. *J. Cell Biol.* 109:1229–1243.
Lefcort, F., and D. Bentley. 1987. Pathfinding by pioneer neurons in isolated, opened and mesoderm-free limb buds of embryonic grasshoppers. *Dev. Biol.* 119:466–480.
Letourneau, P. 1975. Cell-to-substratum adhesion and guidance of axonal elongation. *Dev. Biol.* 44:92–101.
Letourneau, P. C. 1983. Differences in the organization of actin in the growth cones compared with the neurites of cultured neurons from chick embryos. *J. Cell Biol.* 97:963–973.
Letourneau, P. C., and T. A. Shattuck. 1989. Distribution and possible interactions of actin-associated proteins and cell adhesion molecules of nerve growth cones. *Development (Camb.).* 105:505–519.
Lewis, S. A., I. E. Ivanov, G.-H. Lee, and N. J. Cowan. 1989. Organization of microtubules in dendrites and axons is determined by a short hydrophobic zipper in microtubule-associated proteins MAP2 and tau. *Nature (Lond.).* 342:498–505.
Luby-Phelps, K., F. Lanni, and D. L. Taylor. 1988. The submicroscopic properties of cytoplasm as a determinant of cellular function. *Annu. Rev. Biophys. Biophys. Chem.* 17:369–396.
Marsh, L., and P. C. Letourneau. 1984. Growth of neurites without filopodial or lamellipodial activity in the presence of cytochalasin B. *J. Cell Biol.* 99:2041–2047.
Matus, A. 1990. Microtubule-associated proteins. *Curr. Opin. Cell Biol.* 2: 10–14.
Meininger, V., and S. Binet. 1989. Characteristics of microtubules at the different stages of neuronal differentiation and maturation. *Int. Rev. Cytol.* 114:21–79.
Mitchison, T. J., and M. W. Kirschner. 1985. Properties of the kinetochore in vitro. II. Microtubule capture and ATP-dependent translocation. *J. Cell Biol.* 101:766–777.
Mitchison, T., and M. Kirschner. 1988. Cytoskeletal dynamics and nerve growth. *Neuron.* 1:761–772.
Mitchison, T., L. Evans, E. Schulze, and M. Kirschner. 1986. Sites of microtubule assembly and disassembly in the mitotic spindle. *Cell.* 45:515–527.
Mizushima-Sugano, J., T. Maeda, and T. Miki-Noumura. 1983. Flexural rigidity of singlet microtubules estimated from statistical analysis of their contour lengths and end-to-end distances. *Biochim. Biophys. Acta.* 755:257–262.
Morales, M., and E. Fifkova. 1989. Distribution of MAP2 in dendritic spines and its colocalization with actin. *Cell Tissue Res.* 256:447–456.
O'Connor, T., J. Duerr, and D. Bentley. 1990. Pioneer growth cone steering decisions mediated by single filopodial contacts in situ. *J. Neurosci.* 10:3935–3946.
O'Leary, D. D., and T. Terashima. 1988. Cortical axons branch to multiple subcortical targets by interstitial axon budding: implications for target recognition and "waiting periods". *Neuron.* 1:901–910.
Reichardt, L. F., and K. J. Tomaselli. 1991. Extracellular matrix molecules and their receptors: functions in neural development. *Annu. Rev. Neurosci.* 14:531–570.
Reinsch, S. S., T. J. Mitchison, and M. W. Kirschner. 1991. Microtubule polymer assembly and transport during axonal elongation. *J. Cell Biol.* 115: 365–379.
Rudolph, J. E., M. Kimble, H. D. Hoyle, M. A. Subler, and E. C. Raff. 1987. Three *Drosophila* beta-tubulin sequences: a developmentally regulated isoform (B3), the testes-specific isoform (B2), and an assembly-defective mutation of the testes-specific isoform (B2t8) reveal both an ancient divergence in metazoan isotypes and structural constraints for beta-tubulin function. *Mol. Cell Biol.* 7:2231–2242.
Sammak, P., and G. Borisy. 1988. Detection of single fluorescent microtubules and methods for determining their dynamics in living cells. *Cell Motil. Cytoskeleton.* 10:237–245.
Smith, S. J. 1988. Neuronal cytomechanics: the actin-based motility of growth cones. *Science (Wash. DC).* 242:708–715.
Snow, P. M., N. H. Patel, A. L. Harrelson, and C. S. Goodman. 1987. Neural-specific carbohydrate moiety shared by many surface glycoproteins in Drosophila and grasshopper embryos. *J. Neurosci.* 7:4137–4144.
Taghert, P. H., M. J. Bastiani, R. K. Ho, and C. S. Goodman. 1982. Guidance of pioneer growth cones: filopodial contacts and coupling revealed with an antibody to lucifer yellow. *Dev. Biol.* 94:391–399.
Tanaka, E., and M. Kirschner. 1991. Microtubule behavior in the growth cones of living neurons during axon elongation. *J. Cell Biol.* 115:345–363.
Tessier-Lavigne, M., and M. Placzek. 1991. Target attraction: are developing axons guided by chemotropism? *Trends Neurosci.* 14:303–310.
Tosney, K., and L. Landmesser. 1985. Development of the major pathways for neurite outgrowth in the chick hindlimb. *Dev. Biol.* 109:193–214.
Troutt, L. L., and B. Burnside. 1988. The unusual microtubule polarity in teleost retinal pigment epithelial cells. *J. Cell Biol.* 107:1461–1464.
Tsui, H. T., K. L. Lankford, H. Ris, and W. L. Klein. 1984. Novel organization of microtubules in cultured central nervous system neurons: formation of hairpin loops at ends of maturing neurites. *J. Neurosci.* 4:3002–3013.
Westerfield, M., and J. Eisen. 1988. Common mechanisms of growth cone guidance during axonal pathfinding. *In* From Message to Mind. S. S. Easter, K. F. Barald, and B. M. Carlson, editors. Sinauer Associates, Inc., Sunderland, MA. 110–120.